

## The Effect of Land Use on Land Surface Temperature Based on Remote Sensing Indices and GIS in Al-Jouf Northwest, KSA

Amal Yahya Alshaikh

Department of Geography and GIS Faculty of Faculty of Arts and Humanities, King AbdulAziz University, Jeddah KSA

Email: [ayalshikh@kau.edu.sa](mailto:ayalshikh@kau.edu.sa)

**Abstract:** This research has been undertaken to investigate the effect of land Use (LU) on land surface temperature (LST) in Al-Jouf area by using remote sensing indices and (GIS) technique. The study also aims to analyze and compare the relationship between land surface temperature and NDVI / NDWI. The main source of this study is Remote Sensing Data from Landsat-8 OLI (30m resolution) acquired in September (2014). Remotely sensed thermal infrared (TIR) bands have been used to interpret the distribution and changes in surface temperature. Results showed high correlation between Land Surface Temperature and land use types. High temperature values are associated with bare land and built-up area, while low ranges are found in water bodies and vegetation cover. Results also indicate that, LST and [NDVI / NDWI] shared an inverse relationship, implying that an increase in vegetation cover and water bodies abundance would generally reduce land surface temperatures. Generally the LST ranged from 27 °C to 48°C in the study area.

[Amal yahya Alshaikh. **The Effect of Land Use on Land Surface Temperature Based on Remote Sensing Indices and GIS in Al-Jouf Northwest, KSA.** *Life Sci J* 2015;12(9):1-11]. (ISSN:1097-8135). <http://www.lifesciencesite.com>. 1

**Keywords:** Al-Jouf, Land Use, Land Surface Temperature, Effect, Remote Sensing, GIS.

**Abbreviations:** (MNDWI) Modified Normalized Difference Water Index, (NDVI) Normalized Difference Vegetation Index, (LST) Land Surface Temperature, (GIS) Geographic Information Systems, (OLI) Operational Land Imager, (DN) Digital Number, (TIRS) Thermal Infrared Sensor, (LU) Land Use, (NBI) New Built-up Index, (NDSI) Normalized Difference Soil Index.

### Introduction

Land use types plays an important role for the interpretation and distribution of Surface Temperature, The changes in Land use types leads to a change in the Land Surface Temperature, due to the high correlation between LST and Land use. Land surface temperature (LST) is temperature of the skin surface of land which can be derived from satellite information or direct measurements [1]. Land surface temperature (LST) is an important indicator for monitoring the changing of earth resources and one of the most critical parameters in the physical process of surface energy and water balance at local and global scales [2]. Land surface temperature (LST) retrieval is a key issue in infrared quantitative remote sensing [3]. Integration of remote sensing and GIS provides new capability for producing reliable land use / cover map [4]. Remote-sensing data play an increasingly important role in LULC modeling [5]. The information in remotely sensed images plays an important role in environmental monitoring, disaster forecasting, survey, and other applications [6]. The availability of remote sensing data greatly helped mapping and managing earth resources, but its contribution in assessment of temporal changes has been widely used and proved beneficial [7]. Remotely sensed thermal infrared (TIR) bands were used to

extract Land Surface Temperature (LST) values. The main purpose of the research was to analyze the effect of land use on land surface temperature Based on Remote Sensing Indices.

### Study Objectives

This study aims to analyze the effect of land use on land surface temperature based on remote sensing indices and GIS, using landsat-8 OLI imagery, As well as to identify the relationship between [LST] and [NDVI/ NDWI].

### Study Area

Study area includes part of the Al-Jouf region. Al-Jouf is located in the north of the country bordering Jordan [Fig.1]. The province covers an area of 100,212 km<sup>2</sup>, with 361,676 populations. The province includes three governorates: Sakakah, Al-Qurayyat and Dumatal-Jandal [8]. Extents between (37° 03' 02"- 41° 53' 46") N and (28° 32' 08"- 31° 43' 15") E. The terrain have an elevation ranging from (450- 1000m) above sea-level [Fig.2].

### Data Used

In this study the main data source is satellite remote sensing data from "Landsat\_8" [Fig.3], provided by NASA Land Processes Distributed Active Archive Center (LP DAAC), respectively the U.S. Geological Survey (USGS). The Landsat 8 carries two

instruments: the Operational Land Imager (OLI), collects image data for nine shortwave spectral bands (OLI1~ OLI9) over a 185 km swath with a 30 m spatial resolution for all bands except a 15 m panchromatic band (OLI8); the Thermal Infrared Sensor (TIRS),

collects image data for two thermal bands (TIRS10, TIRS11) with a 100 m resolution over a 185 km swath [9]. The study data were taken from 20 September 2014 for Landsat 8 in a scene (path 171, row 039).

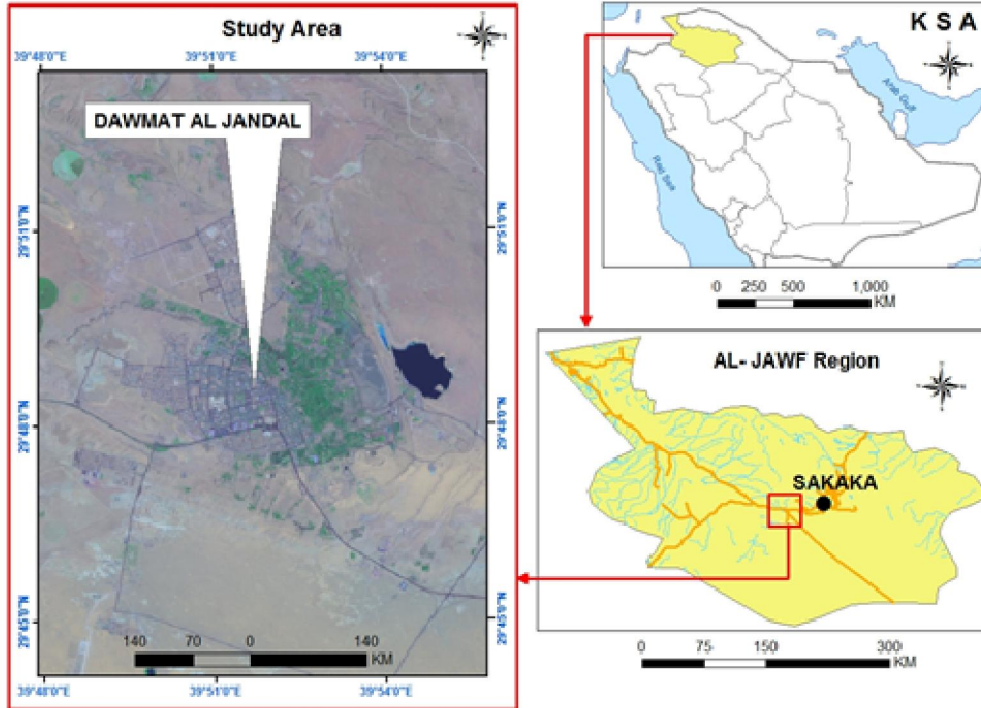


Fig 1. Location of the Study Area

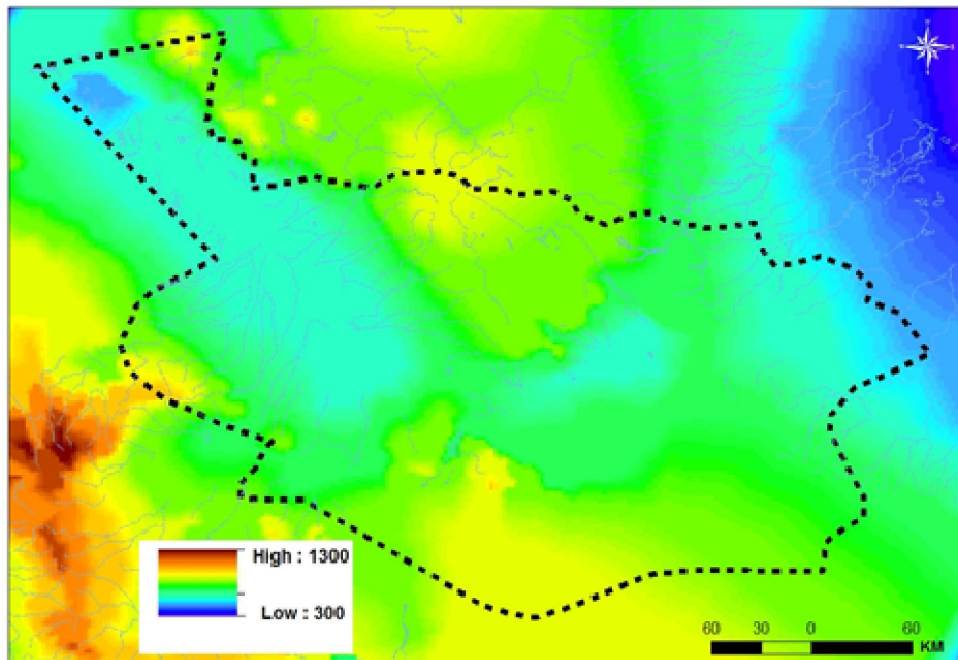


Fig.2. Surface elevation of the study area

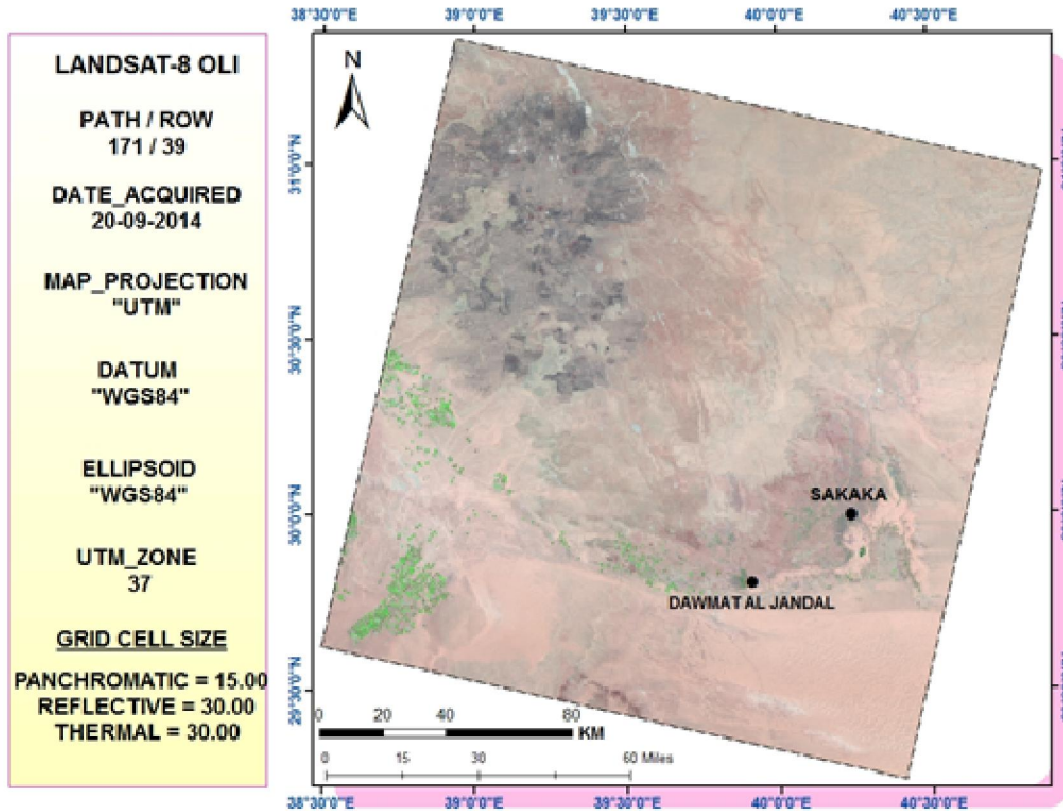


Fig.3. Landsat 8 in a scene (path 171, row 039)

**Methodology**

This study focusing to the analysis effect of Land Use on Land Surface Temperature Based on Remote Sensing Indices [NDVI, NDWI, BAI, NDSI and LST]. Erdas Imagine 2013 and ArcGIS 10.0 software were used, Erdas Imagine 2013 was used for image processing and application remote sensing Indices to extract the value of [NDVI, NDWI, BAI, NDSI and LST], ArcGIS 10.0 software was used for the final output of the results [analysis and map composition]. [Fig.4] Methodological framework showing steps of processing of Landsat thermal satellite data and analysis of [LST], and showing also extraction of land use types using Remote Sensing Indices.

**Extraction Vegetation Cover:**

The red band (0.630–0.680 μm) band 4 and near-infrared band (0.845–0.885 μm) band5 of the landsat-8 sensor was used to calculate [NDVI] values over the study area as in the following equation.

$$NDVI = (NIR - Red) / (NIR + Red) \dots [10]$$

**Extraction Water Bodies:**

The green band (0.525–0.600 μm) band 3 and [Mid-IR] band 6 (1.560–1.660 μm) band 6 of the landsat-8 (OLI) sensor was used to calculate [NDWI] values over the study area as in the following equation:

$$MNDWI = (Green - MIR) / (Green + MIR) [11]$$

**Extraction Land Surface Temperature:**

To extract the surface temperature, three main steps were followed:

The thermal band (10.6-11.2 μm) (band 10) of the Landsat-8 (OLI) sensor was used to derive [LST] over the study area, the following formula was used to *conversion from digital number (DN) to spectral radiance*:

$$L = (Lmin + (Lmax-Lmin) * DN / 255) \dots [12]$$

Where: L = Spectral Radiance. LMIN = (Spectral radiance of DN value 1). LMAX = (Spectral radiance of DN value 255). DN = Digital Number

The next step is used to *Conversion of Spectral Radiance to Temperature in Kelvin* by The following formula:

$$T = \frac{K2}{\ln\left(\frac{K1}{L_\lambda} + 1\right)} \dots [13]$$

Where: T = Effective at-satellite temperature in Kelvin.

K2 = Calibration constant 2. K1 = Calibration constant 1 [table.1]

The next step is used to *Conversion of Kelvin to Celsius*:  $TB = T \text{ (Kelvin)} - 273 \dots$  [14]

Table 1. Calibration Constants of the Thermal Band and (Lmax - Lmin) values

	Constant 1- K1 watts/ (meter squared * ster * μm)	Constant 2 - K2	LMIN	LMAX
Landsat-8 OLI P/R-171/39 (20-09-2014)	774.89	1321.08	0.100	22.001

**Extraction Built-Up Area:**

The [Mid-IR] band (1.560–1.660 μm) band 6, [Mid-IR] (2.100–2.300 μm) band 7 and green band (0.525–0.600 μm) band 3 of the Landsat-8 (OLI) sensor was used to derive [NBAI] over the study area as in the following equation.

$$NBAI = (Mid-IR - Mid-IR / green) / (Mid-IR + Mid-IR / green) \dots$$
 [15].

**Extraction soil index:**

The [SWIR2] band (2.100–2.300 μm) band 7, [TIR] band (10.6-11.2 μm) (band 10) of the Landsat-8 (OLI) sensor was used to derive [NDSI] over the study area as in the following equation.

$$NDSI = (TIR - SWIR2) / (TIR + SWIR2) \dots$$
 [16].

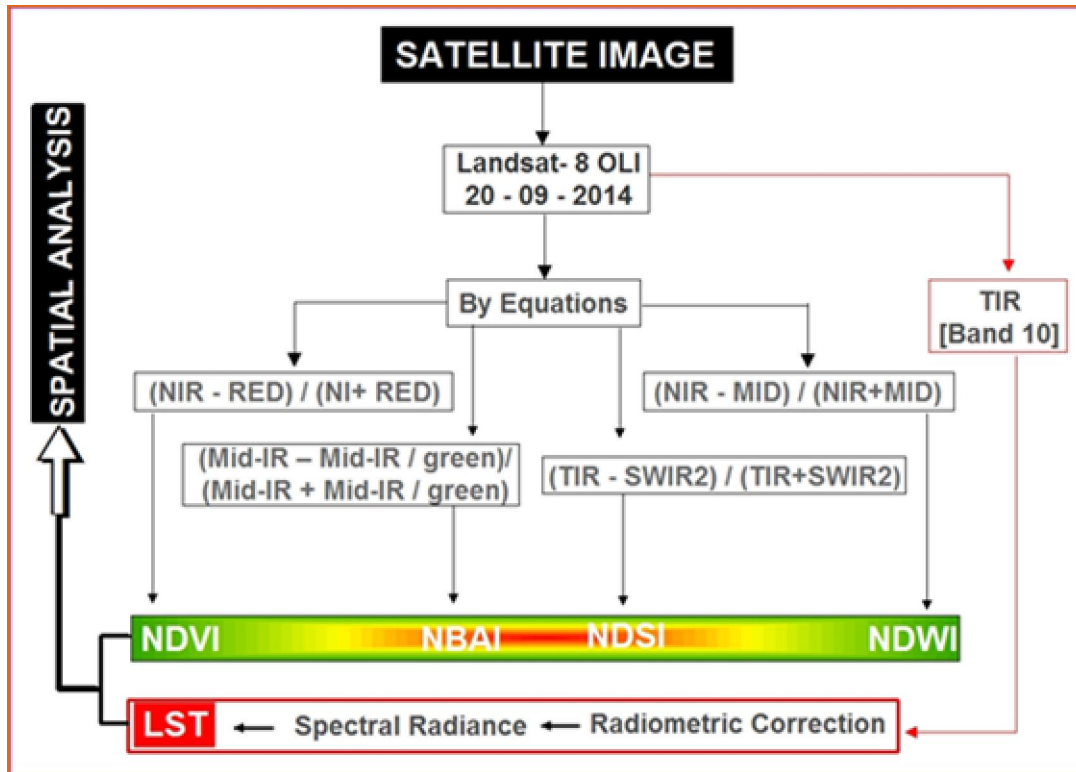


Fig. 4. Methodology frame work

**Results and Analysis**

In this study, image processing and GIS analysis were used to extraction [NDVI, NDWI, BAI, NDSI and LST] and composition the map of the land use and spatial analysis of the results.

Figure 5 shows extracted [NDVI, NDWI, BAI, and LST].

Figure 6 shows (**Land Use Map**) that has been extracted from landsat\_8 based on Remote Sensing Indices. The land use types can be divided into five categories in the study area, namely: Water, vegetation, built-up area, sands and barren land.

Figure 7 shows water bodies (Blue Color) Like NDVI, NDWI has a native scaling of [-1 to +1] The

Normalized Difference Water Index was computed from landsat reflectance data using Green and MID bands. NDWI values ranged from (-0.362518 - 0.48529). Results also have shown that The Lower [LST] value within water area is 27°C, and the highest [LST] value within water area is 31°C.

Figure.8 shows vegetation cover (Green Color) NDVI values range from [-1 to 1]. Vegetated areas will generally yield high values because of their relatively

high near-infrared reflectance and low visible reflectance. The Normalized Difference Vegetation Index was computed from landsat reflectance data using NIR and RED bands. In this study, NDVI values ranged from (-0.361558 - 0.499315). Results also have shown that The Lower [LST] value within vegetation area is 31°C, and the highest [LST] value within vegetation area is 38°C.

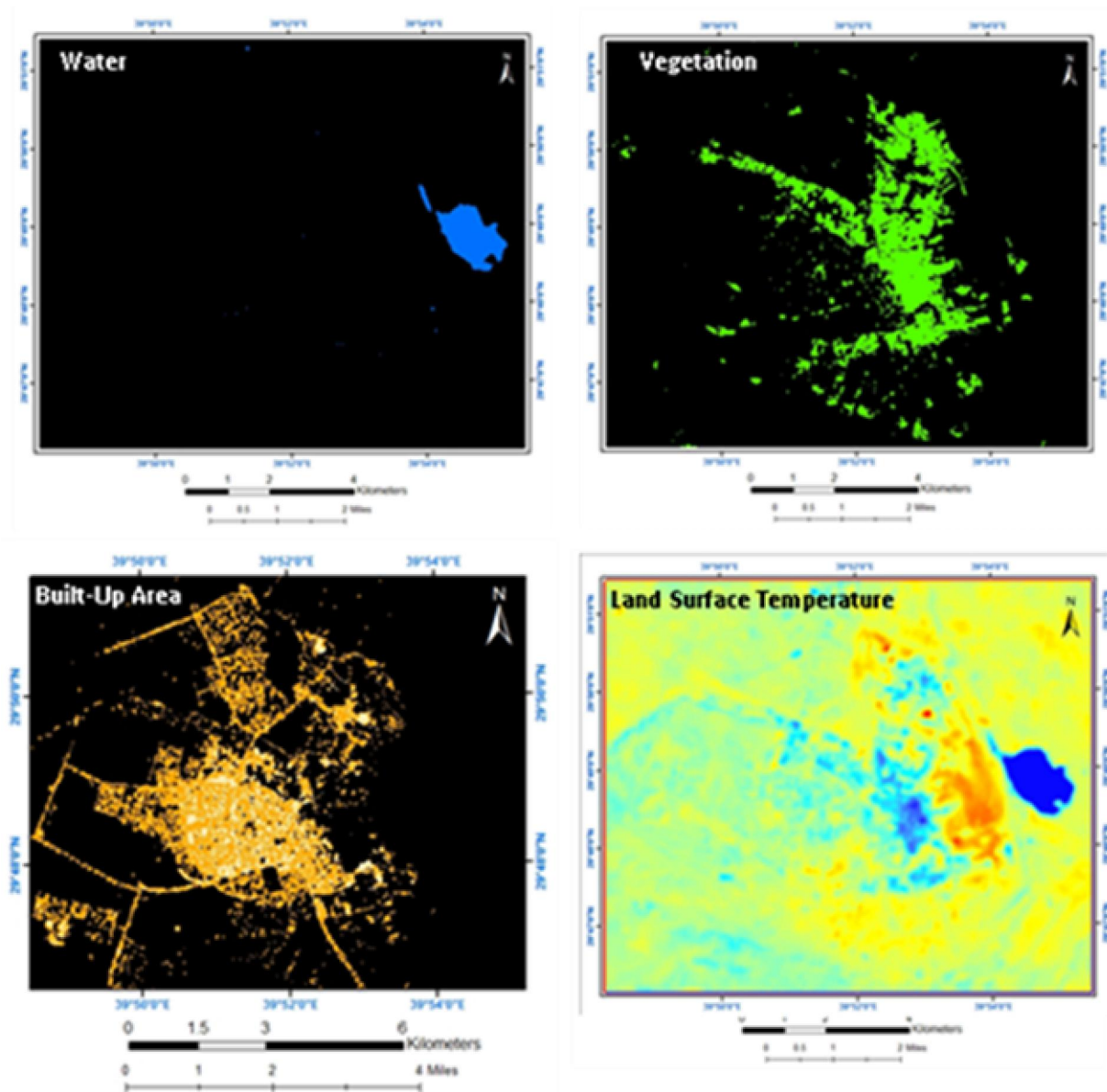


Fig. 5. Extracted [NDVI, NDWI, BAI, and LST] 20-09-2014

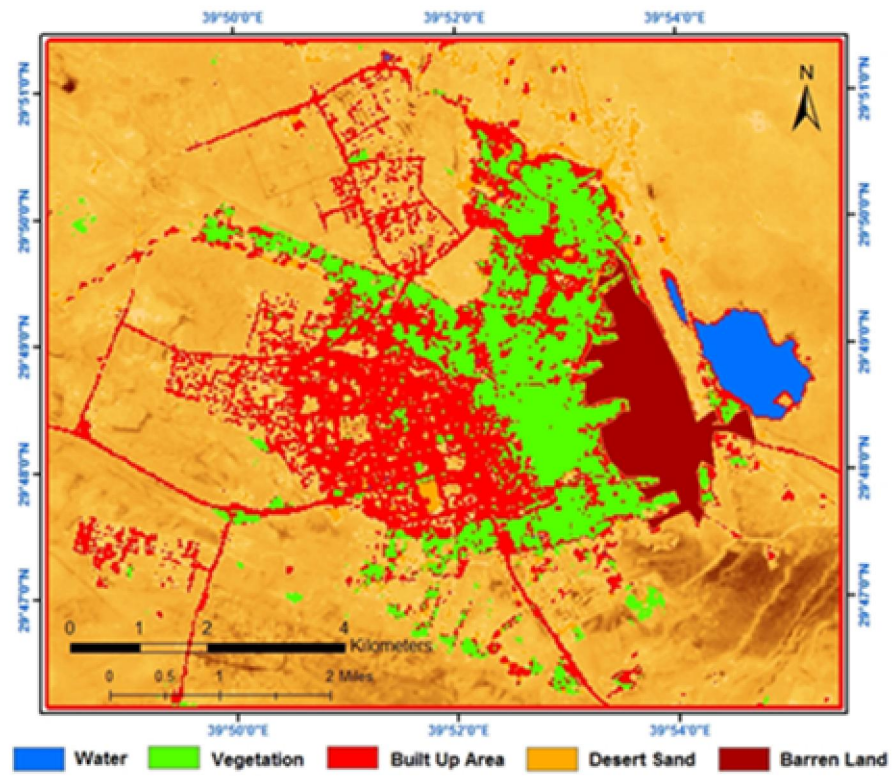


Fig. 6. Land use map

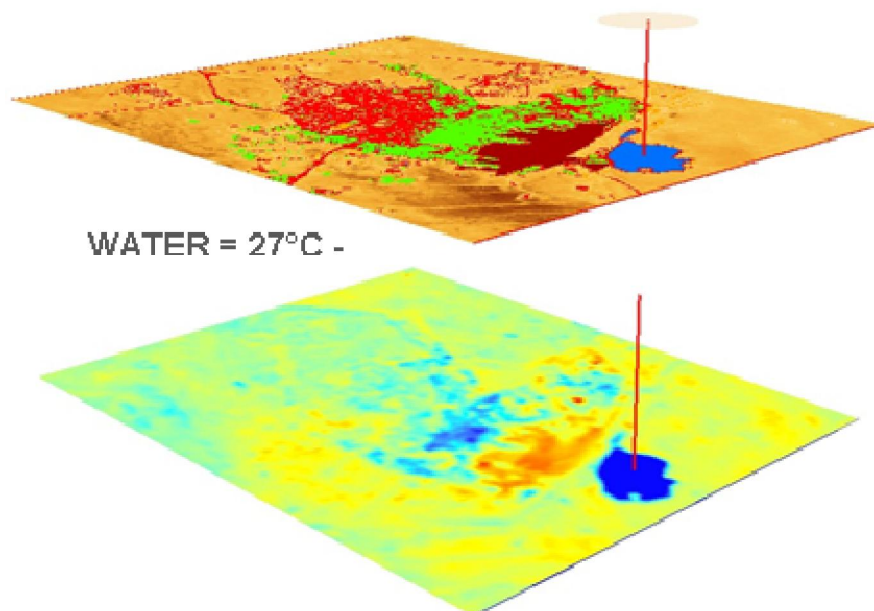


Fig. 7. LST within water bodies area

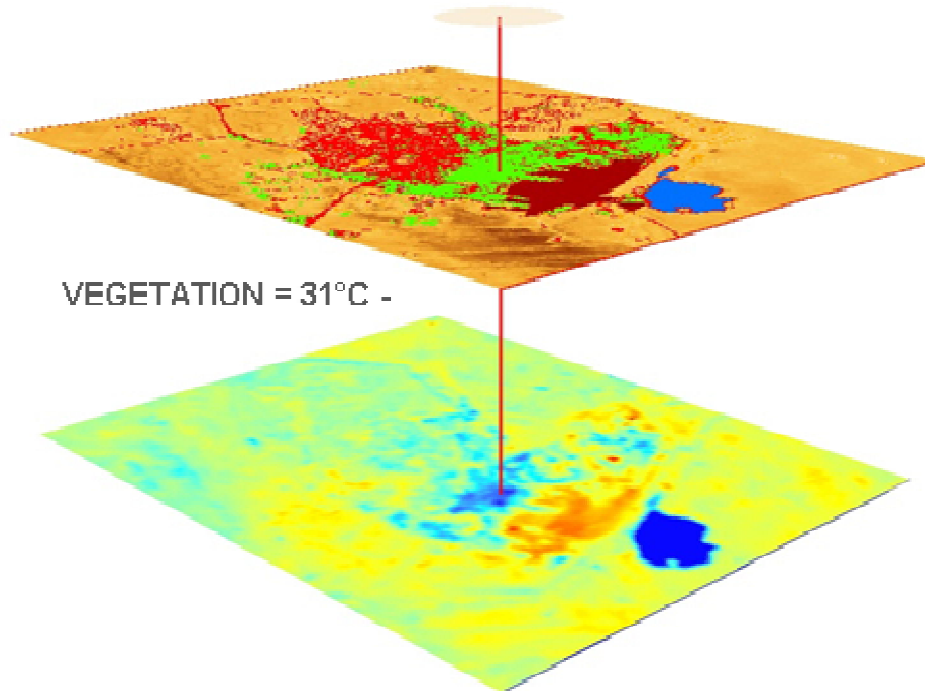


Fig. 8. LST within vegetation cover area

Figure 9 shows built-up area (Red Color). Values of Normalized Difference built-up area was computed from landsat reflectance data using Green and MID bands. NBAI values ranged from (-0.419164-0.515069). Results also have shown that The Lower

[LST] value within water area is 38°C, and the highest [LST] value within water area is 42°C.

The LST values are lower in Vegetation areas within built-up area while they become high in Vegetation-free Areas Throughout the built-up area.

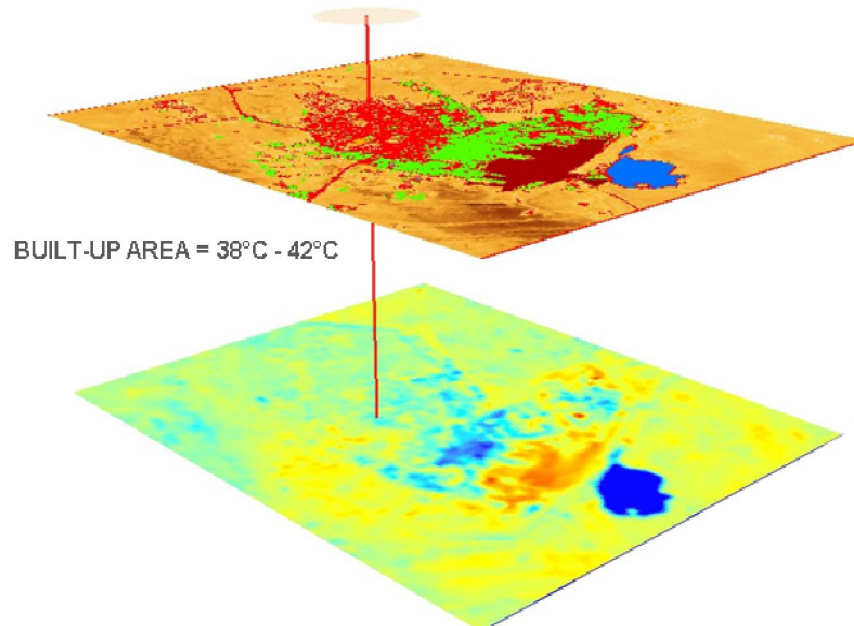


Fig. 9. LST within built-up area

Figure.10 shows sands areas (Light brown color). A value of soil index was computed from landsat reflectance data using Thermal and MID bands. Results

also have shown that The Lower [LST] value within water area is 42°C, and the highest [LST] value within water area is 44°C.

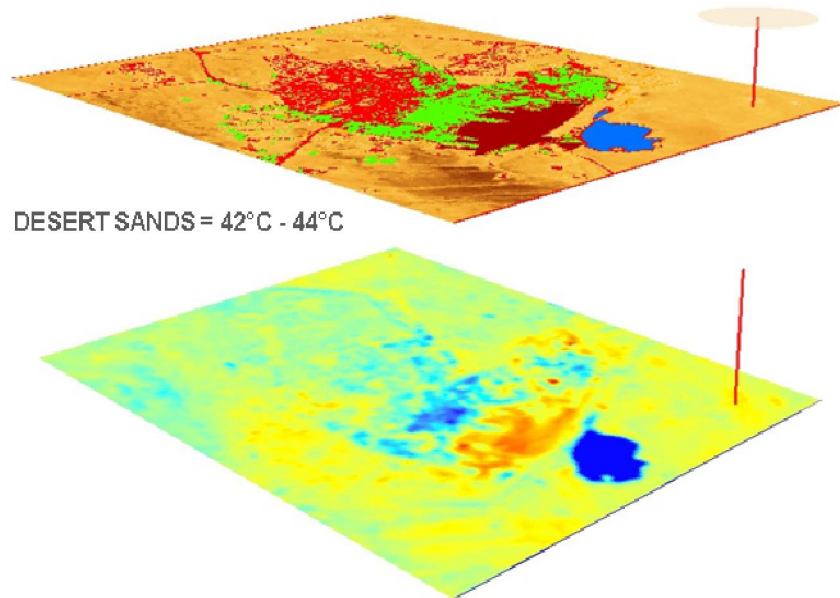


Fig. 10. LST within desert sands area

Figure.11 shows barren land (Dark brown color). A value of barren Index was computed from landsat reflectance data using Thermal and MID bands. Sometimes it's very difficult to separate barren land and built-up areas because of their similar spectral

character in Landsat-8 imagery, so it's needs to manually select. Therefore, it relies to some degree on the experience and skill of the image analyst. Results also have shown that The Lower [LST] is 44°C, and the highest [LST] value is 48°C.

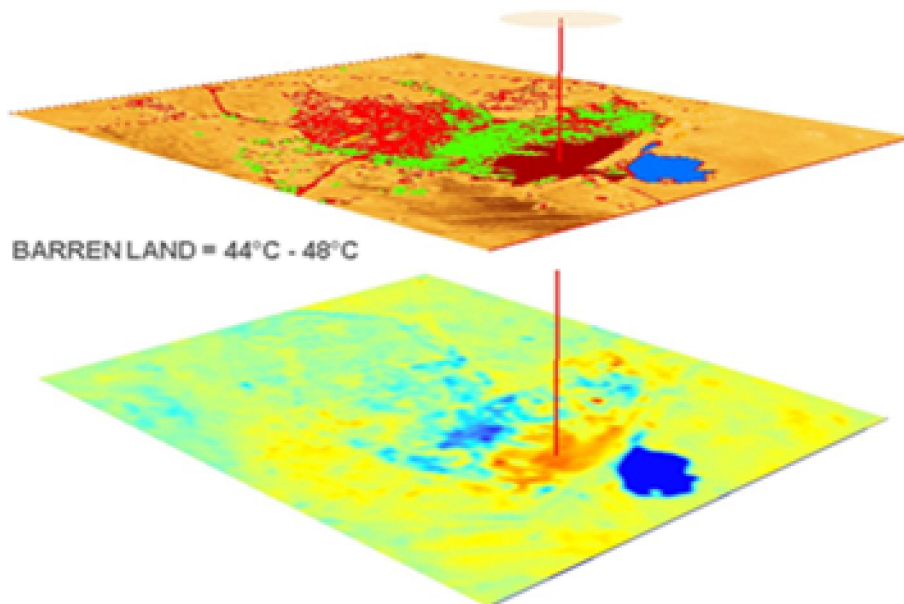


Fig. 11. LST within barren land area

Fig. 12 and Table 2 shows that there was strong negative relationship between LST and water bodies / vegetation cover an analysis based on linear regression showed that the coefficient of determination value ( $R^2$ ) was (0.745) and (0.604) respectively.

Implying that an increase in vegetation cover and water bodies abundance would generally reduce land surface temperatures.

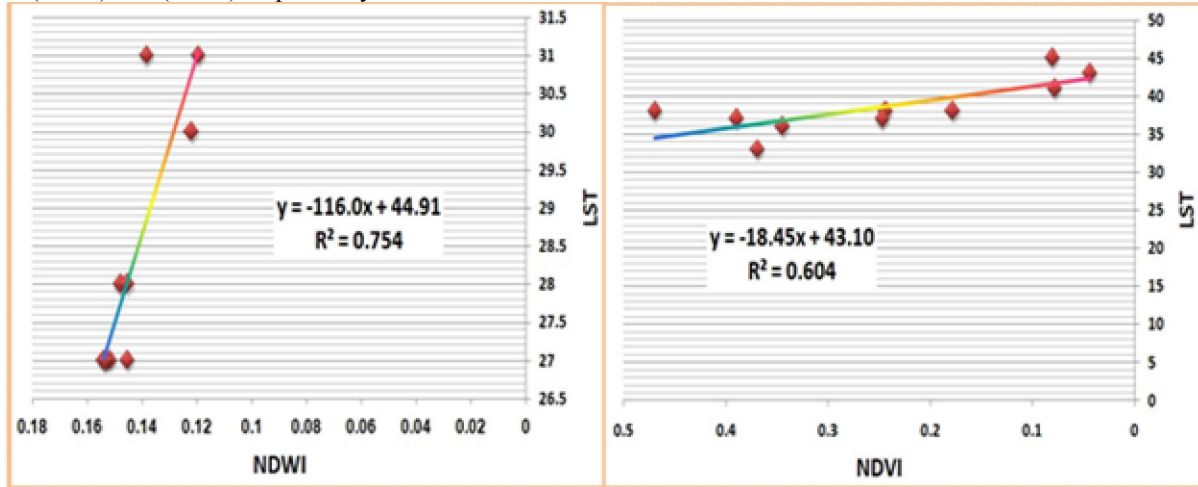


Fig. 12. Correlation coefficient between LST and NDWI/NDVI

Table 2. Relationship between LST and NDWI/NDVI

Num	Latitude	longitude	MNWI	LST
1	39°54'39.613"E	29°48'49.458"N	0.154116	27
2	39°54'58.474"E	29°48'58.441"N	0.119582	31
3	39°54'45.431"E	29°48'31.317"N	0.147945	28
4	39°54'40.462"E	29°48'51.867"N	0.151816	27
5	39°54'30.404"E	29°48'47.988"N	0.145512	27
6	39°54'37.131"E	29°48'43.533"N	0.153297	27
7	39°54'56.061"E	29°48'40.184"N	0.145582	28
8	39°54'44.637"E	29°48'45.385"N	0.153520	27
9	39°55'7.308"E	29°48'47.68"N	0.138429	31
10	39°55'1.688"E	29°48'55.402"N	0.122090	30

Num	Latitude	longitude	NDVI	LST
1	39°52'38.501"E	29°50'20.266"N	0.468986	38
2	39°53'5.116"E	29°50'1.602"N	0.243681	38
3	39°53'14.069"E	29°49'59.614"N	0.178088	38
4	39°53'38.299"E	29°49'20.427"N	0.080645	45
5	39°52'33.286"E	29°49'2.357"N	0.246597	37
6	39°52'21.06"E	29°49'13.201"N	0.344444	36
7	39°52'12.14"E	29°49'11.248"N	0.078426	41
8	39°52'2.11"E	29°49'9.167"N	0.043855	43
9	39°52'51.959"E	29°48'29.09"N	0.368938	33
10	39°52'22.955"E	29°48'29.174"N	0.389470	37

**Conclusion**

1. Land use plays an important role in the ecosystem, and it could be the reason of variation in the Land Surface Temperature [Fig.13].
2. Remote-sensing data play an increasingly important role in land use modeling.
3. The abundance of water and vegetation is one of the most influential in controlling (LST), where is observed the large variability between (LST) values

- and (NDVI/ NDWI) for each pixel in the image of the locations that were selected in the study area [Table.3].
4. Study have proved that there was strong negative relationship between LST and water bodies / vegetation cover
5. Table.4 Drawing conclusions from analyzing Correlation Coefficient between (W/V) and (LST).
6. Fig.14 Drawing conclusions from analyzing Trend change of LST.

Table 3. The Variation in LST based on the types of land use

	WATER	VEGETATION	BUILT-UP AREA	SANDS	BARREN LAND
LST	27°C - 31°C	31°C - 38°C	38°C - 42°C	42°C - 44°C	44°C - 48°C
Average	29°C	34	40°C	43°C	46°C

Table 4. Correlation Coefficient between (W/V) and (LST)

	WATER	VEGETATION
R	-0.377	-0.302
R <sup>2</sup>	0.754	0.604

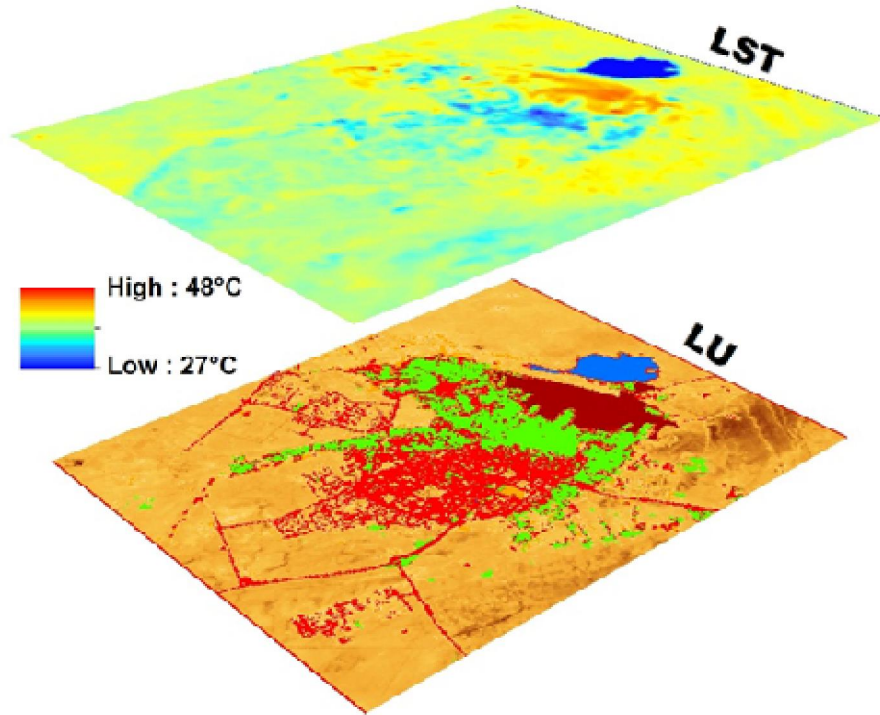


Fig. 13. Effect LU on LST

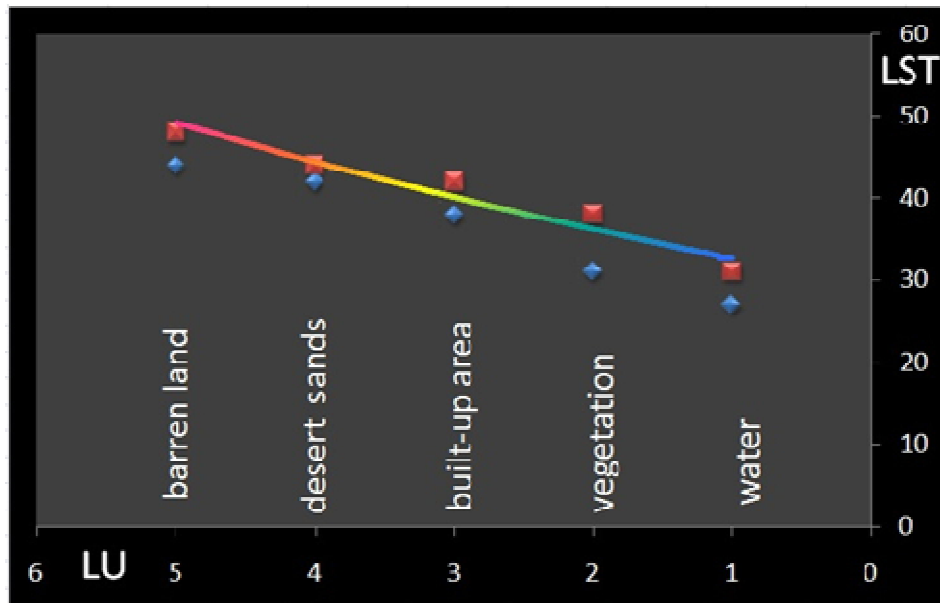


Fig.14. Trend change of LST

**References**

1. Soheila Youneszadeh Jalili 2013. The effect of land use on land surface temperature in the Netherlands. MSc thesis Lund University GEM thesis series nr 1.
2. Enyu Zhao, Yonggang Qian, Caixia Gao, Hongyuan Huo, Xiaoguang Jiang and Xiangsheng Kong 2014. Land Surface Temperature Retrieval Using Airborne Hyperspectral Scanner Daytime Mid-Infrared Data. *Remote Sens.* 2014, 6(12), 12667-12685; doi:10.3390/rs61212667.
3. WAN Z., Y. ZHANG and Q. ZHANG (2004). Quality assessment and validation of the MODIS global land surface temperature. *INT. J. REMOTE SENSING*, 10, VOL. 25, NO. 1, 261–274.
4. Ali, R.R. and Shalaby, A. (2012). Response of Topsoil Features to the Seasonal Changes of Land Surface Temperature in the Arid Environment. *International Journal of Soil Science*, 7 (2): 39-50.
5. Jensen J. R 1983. Biophysical Remote sensing – Review Article. *Annals of the Associations of American Geographers*, t. 73, nr 1, pp. 111-132.
6. Tingting Liu, Liangpei Zhang Pingxiang Li and Hui Lin 2012. Remotely sensed image retrieval based on region-level semantic mining.
7. Mirza Muhammad Waqar, Johum Fatimah Mirza, Rafia Mumtaz and Ejaz Hussain 2012. Development of New Indices for Extraction of Built-Up Area & Bare Soil from Landsat Data. <http://www.moi.gov.sa/wps/portal/jowf>.
9. S. Li, X. Chen 2014. A NEW BARE-SOIL INDEX FOR RAPID MAPPING DEVELOPING AREAS USING LANDSAT 8 DATA.
10. Rouse, J.W.; Haas, R.H.; Schell, J.A.; Deering, D.W. Monitoring Vegetation Systems in the Great Plains with ERTS (Earth Resources Technology Satellite). In *Proceedings of Third Earth Resources Technology Satellite Symposium*, Greenbelt, ON, Canada, 10–14 December 1973; Volume SP-351, pp. 309–317.
11. Xu, H. Modification of normalised difference water index (NDWI) to enhance open water features in remotely sensed imagery. *Int. J. Remote Sens.* 2006, 27, 3025–3033.
12. NASA, (2011). *Landsat 7 Science Data User's Handbook*.
13. Lwin, K (2010). Estimation of Landsat TM Surface Temperature Using ERDAS Imagine Spatial Modeler. SIS Tutorial Series. Copyright © 2010 by Division of Spatial Information Science. <http://giswin.geo.tsukuba.ac.jp/sis/tutorial/koko/SurfaceTemp/SurfaceTemperature.pdf>.
14. Yuji Murayama 2010. Estimation of Landsat TM Surface Temperature Using ERDAS Imagine Spatial Modeler, Division of Spatial Information Science Graduate School of Life and Environmental Sciences, University of Tsukuba.
15. Jun Zhang, Peijun Li and Jinfei Wang (2014). Urban Built-Up Area Extraction from Landsat TM/ETM+ Images Using Spectral Information and Multivariate Texture. *Remote Sens.* 2014, 6, 7339-7359.
16. Yuji Murayama, (2010). Estimation of Landsat TM Surface Temperature Using ERDAS Imagine Spatial Modeler, Division of Spatial Information Science Graduate School of Life and Environmental Sciences, University of Tsukuba.

9/8/2015